GW4869 can inhibit epithelial-mesenchymal transition promoted by extracellular HSP90α in EGFR-mutated NSCLC cells

Xuan Wan
Nanfang Hospital, Southern Medical University
Jiangzhou Du
Nanfang Hospital, Southern Medical University
Yuting Fang
Southern Medical University
Danhui Huang
Nanfang Hospital, Southern Medical University
Hangming Dong
Nanfang Hospital, Southern Medical University
Shaoxi Cai (hxkc@smu.edu.cn)
Nanfang Hospital, Southern Medical University

Article

Keywords:

Posted Date: July 6th, 2022

DOI: https://doi.org/10.21203/rs.3.rs-1783485/v1

Abstract

Non-small cell lung cancer (NSCLC) is the most common subtype of lung cancer with the high morbidity and mortality in the world. Meanwhile, the acquired drug resistance against EGFR-mutated NSCLC is increasingly serious. HSP90α might play critical roles in NSCLC, but the effect of GW4869 on extracellular HSP90α remains unclear. We collected plasma samples from 22 NSCLC and 10 healthy individuals, and measured the plasma HSP90α levels by ELISA. Western blot was used to detect the levels of HSP90α, E-cadherin, N-cadherin, and Vimentin in HCC827 and PC9 cells. We found that extracellular HSP90α was upregulated in NSCLC mutated patients and accelerated epithelial-mesenchymal transition (EMT) and invasion/migration capacity in EGFR-mutated NSCLC cells. Meanwhile, we also confirmed that GW4869 inhibited the expression of eHSP90α, EMT and invasion/migration abilities in HCC827 and PC9, and enhanced the antitumor activity of gefitinib in BALB/C nude mice in vivo. These studies suggest that GW4869 can inhibit epithelial-mesenchymal transition promoted by extracellular HSP90α in non-small cell lung cancer, which provides new strategies for delaying the development of acquired resistance to gefitinib for EGFR-mutated NSCLC.

Introduction

Lung cancer is the most common cancer of both sexes with an estimated 2.2 million new cancer cases and 1.8 million deaths per year[1]. Histologically, 85% of lung cancer cases are defined as non-small cell lung cancer (NSCLC). In Asia, approximately 50% of NSCLC patients harbor mutations of epidermal growth factor receptor (EGFR)[2], and mainly mutations in exons 18, 19, and 21 of EGFR. EGFR-tyrosine kinase inhibitor (EGFR-TKI), such as gefitinib, an effective drug in the clinical targeted treatment of NSCLC. The initial treatment effect of EGFR-TKI is satisfactory, but later patients tend to develop acquired resistance[3]; [4], which is not conducive to the later treatment of patients with EGFR-mutated NSCLC. Therefore, delaying or overcoming the onset of acquired drug resistance and optimizing the treatment strategies for EGFR-TKI resistance is the key to solve drug resistance in NSCLC[5-7].

Epithelial-mesenchymal transition (EMT) is a vital process driving the development of drug resistance in NSCLC[8]. Previous reports have shown that tumor cells with EMT are more likely to develop drug resistance[9]. In addition to secondary mutations on EGFR or EGFR amplifications, EMT is also one of main resistance mechanisms to EGFR-TKI with alteration in EMT-gene signatures and specific markers of the mesenchymal phenotype[10]. During the EMT process, epithelial cells lose their adhesion capacity and acquire mesenchymal features, as well as increased behavioral-dynamic abilities of migration and invasion[11], represented with down-regulation of E-cadherin and up-regulation of Vimentin and N-cadherin[12].

Heat shock protein 90α (HSP90α) is a highly conserved molecular chaperone that mediates the stability of protein structure by participating in the correct folding of the client protein and ensuring its normal physiological function[13].In addition to being localized intracellularly, HSP90α can be excreted into the

extracellular environment, which called as extracellular HSP90α (eHSP90α), under stress such as heat and hypoxia in tumor cells[14].Extracellular HSP90 secreted through exosome and may be a very meaningful target for tumor therapy[15; 16].Cell motility and invasion have been found to be induced by eHSP90 in several cancer cell lines and preclinical models[17].

HSP90 inhibitors have been designed and utilized in clinical trials targeted for HSP90 client applied in mutant EGFR in NSCLC, HER-2 in breast cancer, and targeted HSP90 co-chaperones including HSP40, HSP70 or CDC37 as well as served as an adjuvant to other chemotherapeutics and shut down the heat shock response to increase cellular stress and protein degradation[18]. As well studies reveal that selected sensitivity of cancer cells to HSP90 inhibitors is due to inhibition of the extracellular HSP90 (eHSP90) rather than intracellular HSP90 by these inhibitors. Only the group of “eHSP90-dependent” cancer cells is sensitive to HSP90 inhibitors owing to their utilization of eHSP90 for motility, invasion and metastasis[19]. Notably, it has been shown that HSPs and vesicles were co-released and HSPs served as mediators of Resistance-Associated Secretory Phenotype (RASP)[20].

Inhibitors of extracellular vesicles (EVs) have been categorized into two main groups i.e. those targeted EV trafficking (calpeptin, manumycin A and Y27632) and those targeted lipid metabolism (pantethine, imipramine and GW4869)[21]. Extracellular HSPs and HSP-rich EVs can promote cancer progression by enhancing EMT, migration, invasion, heterogeneity, metastasis, CSC/CIC properties, and drug resistance in cancer cells and angiogenesis[20].

GW4869 is a cell-permeable symmetrical dihydroimidazolamide compound that can be used as an effective, specific and non-competitive inhibitor of membrane-neutral sphinomyelinase (i.e. nSMase2), which prevents the ceramide-modulated inward budding of multivesicular bodies (MVBs) and the subsequent release of exosomes from MVBs[21]. GW4869 has been reported to reduce exosome release and is often used to as exosome inhibitors, which suppresses an increase on exosomes secretion occurred in response to genfitinib and chemoresistance in colorectal, pancreatic and ovarian cancer cells[22; 23]. Meanwhile, GW4869 may be a helpful strategy to overcome the antagonistic effects via inhibition of exosome and miRNA secretion when EGFR-TKIs and chemotherapeutic agents are co-administered[22; 24].

Co-release of EVs and eHSP90 from high oral metastatic cancer and castration-resistant prostate cancer cells induce tumorigenicity and EMT[25], however, in addition to inhibit exosome secretion, the effects of GW4869 on HSP90α expression and EMT in EGFR-mutated NSCLC cells are still unclear. Consequently, we will investigate whether GW4869 can inhibit EMT process promoted by extracellular HSP90α in EGFR-mutated NSCLC cells.

Results

High level of HSP90α in the plasma of NSCLC patients with EGFR mutation. We collected 22 plasma samples from NSCLC patients and 10 plasma samples from healthy individuals. Plasma HSP90α levels

were detected by ELISA. We found that the concentration of plasma HSP90α levels in patients with EGFR-mutated NSCLC (192.8 ± 13.11ng/ml) were significantly higher than those in the control group (72.79 ± 4.545ng/ml) by 2.64-fold (Fig. 1A). This result indicates that HSP90α might be associated with the oncogenesis of NSCLC.

eHSP90α promoted EMT through TGF-β1 induction. To explore the expression of eHSP90α, we detected the levels of extracellular expression of HSP90α and intracellular expression of E-cadherin, N-cadherin and Vimentin in HCC827 and PC9 by western blot. We found that the amount of eHSP90α was upregulated in response to TGF-β1 treatment in a dose-dependent manner in both two cells. Correspondingly, the expression level of E-cadherin decreased while both N-cadherin and Vimentin levels increased (Fig. 1B). The upregulation of eHSP90α induced by TGF-β1 suggests that the expression of eHSP90α may play a role in the occurrence of EMT.

Due to the most effect of stimulation of TGF-β1 in HCC827 is under the concentration of 40ng/ml and PC9 is 20ng/ml,we treated this concentration in the next experiment.Human recombinant HSP0α (hrHSP90α) was then added to the culture medium in the two cells. We found that the expression of E-cadherin in the TGF-β1 of 40ng/ml combined with hrHSP90α in 10μg/ml group was lower than in the TGF-β1 group (40ng/ml) in HCC827, while N-cadherin and Vimentin levels were increased compared with TGF-β1 treatment alone (Fig. 2A). These findings suggest that hrHSP90α can promote TGF-β1-induced EMT. In PC9, the combination of TGF-β1 in 20ng/ml and hrHSP90α in 10μg/ml

We silenced HSP90α with short interfering RNA (siRNA) and found that the expression of E-cadherin in HCC827 was increased compared to the si-control group and decreased after stimulation of TGF-β1. The protein levels of N-cadherin and Vimentin decreased in siHSP90α group compared to the si-control group but increased after TGF-β1 stimulation (Fig. 2B). These results suggested that eHSP90α promoted the occurrence of EMT. The same trend can be seen in the cell of PC9.Therefore, these reveals that eHSP90α facilitated EMT via TGF-β1.

eHSP90α accelerated migration and invasion capacity in EGFR-mutated NSCLC cells. To explore the cell mobility of HCC827 and PC9 promoted by TGF-β1 combined with hrHSP90α, it was detected by wound healing assay. There was no statistical difference between the group of hrHSP90α(21.33 ± 0.62%) and control(18.43 ± 1.18%) in HCC827. However, the cell migration rate of TGF-β1 treatment combined with hrHSP90α(44.91 ± 1.00%) was higher than TGF-β1 alone (28.12 ± 0.53%) (Fig. 3A). In PC9, we cam found that the migration rate of the combination of TGF-β1 and hrHSP90α (67.51 ± 2.08%) is much more than the group of TGF-β1 (36.15 ± 1.00%) and the migration rate of the treatment of hrHSP90α (13.88 ± 1.52%) is also higher than the control group (5.85 ± 0.95%)(Fig. 3B).

Transwell assay was used to detect the cell invasion number by TGF-β1 combined with hrHSP90α. The results showed that the number of cells per field in the TGF-β1 combined with hrHSP90α treatment group was higher than the TGF-β1 alone both in HCC827 (60 ± 4 versus 46.33 ± 5.50) and PC9 (93.33 ± 6.42 versus 73.33 ± 6.65) (Fig. 3C). Meanwhile, the number of hrHSP90α invaded cells was also higher than the control group in HCC827(37.66 ± 2.30 versus 14 ± 5.29) and PC9(47.33 ± 3.78 versus 13.00 ± 3.60).

These results suggest that extracellular HSP90α can promote the migration and invasion of EGFR-mutated NSCLC cells induced by TGF-β1. The ability of migration and invasion in PC9 was stronger than HCC827.

GW4869 inhibited the expression of eHSP90α and EMT. To study the effects of GW4869, treated cells with GW4869. With increasing concentrations of GW4869, we found that expression of eHSP90α decreased significantly compared with the control group ($P < 0.05$) when GW4869 concentration was at 1 nM (Fig. 4A) both in HCC827 and PC9, accompanied with the increase of E-cadherin and the decrease of N-cadherin and Vimentin ($P < 0.05$). Meanwhile, being co-treated with TGF-β1 of 40ng/ml and GW4869 (1nM), we found that GW4869 inhibited the TGF-β1-induced increase in eHSP90α, and reversed the EMT process induced by TGF-β1 (Fig. 4B). In PC9, we carried out with 10ng/ml and 1nM in GW4869 and come to the same trends. These results suggest that the exosome inhibitor GW4869 could inhibit EMT produced by TGF-β1-stimulated cells.

GW4869 inhibited migration and invasion abilities in HCC827 and PC9. To further study the role of GW4869 on EMT, we showed that the cell mobility of TGF-β1 treatment combined with GW4869 (28.33 ± 0.98%) was lower than TGF-β1 treatment (59.04 ± 0.99%) alone (Fig. 5A), as well as GW4869 group (16.77 ± 0.86%) compared with control group(6.21 ± 0.10) through wound healing assay in HCC827. Also in PC9, the migration rate of GW4869 and TGF-β1 group is the lowest (15.19 ± 1.06%)compared to other three groups.They both suggested that GW4869 can inhibit the migration of TGF-β1-stimulated (Fig. 5B). Transwell assay showed that the cell invasion number of GW4869 group (13.33 ± 1.52) was significantly lower than the control (18.66 ± 1.52) in HCC827, while the cell invasion number of TGF-β1 combined with the GW4869 group (35 ± 3) was significantly lower than that of TGF-β1 alone group(50.66 ± 8.14) (Fig. 5C).Also in PC9, the cell invasion number of TGF-β1 combined with the GW4869 group (65.33 ± 4.61) was significantly lower than that of TGF-β1 alone group (80.66 ± 7.02) They both suggested that GW4869 can inhibit the migration and invasion of TGF-β 1-stimulated NSCLC cells.

GW4869 enhanced gefitinib sensitivity in vivo. To further evaluate the effect of GW4869 in EMT and eHSP9α we performed an research *in vivo*. We subcutaneously injected HCC827 cells into BALB/C nude mice. After tumor size reached about 50 mm^3, mice were divided into three groups: Control, Gefitinib, Gefitinib + GW4869(Fig. 6A). By day 28, the significant reduction in tumor size in the group of Gefitinib and Gefitinib + GW4869.Tumor size in the GW4869 + Gefitinib group was the smallest than each other groups (Fig. 6B). The Gefitinib + GW4869 group had the lowest serum HSP90α levels of three groups (Fig. 6C). The same trend in tumor weight was observed (Fig. 6D). IHC analysis also showed that expression of N-cadherin was significantly lower in the Gefitinib + GW4869 compared with each single-drug group, while E-cadherin showed the opposite pattern and calculated by IHC scores (Fig. 6E). To summarize, these results suggested that the combination of gefitinib and GW4869 enhanced gefitinib sensitivity *in vivo*.

Discussion

At present, EMT has been considered one of the important mechanisms for the generation of acquired drug resistance to EGFR-TKIs[10; 26]. The release of HSP90α from tumor cells and its role in promoting cancer cell survival, migration, invasion, and stemness through autocrine mechanisms is well established[27]. However, less is known whether eHSP90α is involved in the development of EMT and how inhibitors mediate EVs and EMT despite eHsp90 is involved in extracellular matrix remodeling, activation of MMP2 and result in invasion and metastasis[27]. The secreted HSP90α attenuates the effect of anticancer drugs in NSCLC cells through AKT/GSK3β/β-catenin signaling pathway[28]. HSP90 inhibitor NVP-AUY922 enhances the radiosensitivity of lung cancer cells with acquired resistance to EGFR-TKIs. As an HSP90 inhibitor, WK88-1 can reduce gefitinib resistance in gefitinib-resistant HCC827 cells[29]. With unsatisfactory clinical results of certain HSP90 inhibitor resulting from HSP90 upregulation, dual-targeting inhibitors could present increased efficiencies and/or lower toxicities and even overcome the anticancer agents-induced drug resistance[30]. As well there are few studies describing the relationship between eHSP90α and EGFR-mutated NSCLC. We constructed cell model of EMT with TGF-β1 in HCC827 and PC9, which were both EGFR-mutated NSCLC cells, and found that eHSP90α was upregulated by TGF-β1 in a concentration-dependent manner, and the development of EMT was inhibited following interference with HSP90α. Meanwhile, exogenous supplementation of hrHSP90α promoted the expression of N-cadherin and Vimentin and the invasion and migration in both cells. These studies suggest that eHSP90α can promote EMT and the invasion and migration in EGFR-mutated NSCLC cells.

Currently, extracellular HSP90 has been found to secret by exosomes and co-released with exosomes as well[17; 25; 31]. Besides, HSP90 membrane-deforming ability promotes exosome release in vitro and vivo while eHSP90 and HSP90-rich EVs function in process of EMT[32]. If we could inhibit the release of eHSP90, it might provide more possibilities against EMT. GW4869 is often used to block exosome production and inhibit exosome release, and is found to reduce inflammation and cardiac dysfunction[33]. GW4869 can inhibit exosomes and then reverse gefitinib resistance and even overcome the antagonistic effects co-administrated with cisplatin in NSCLC, however, its mechanism remains to be further studied[22; 24]. Of note, GW4869 inhibits EMT in lung cancer cells induced by cancer-associated fibroblasts (CAFs) [34], as well as prostate cells[35]. Also, the combination of GW4869 and PD-L1 had the potential to improve the clinical anti-tumor treatment efficacy[36]. Therefore, we explored the role of extracellular HSP90α in EMT, invasion and migration by inhibiting the secretion of exosomes inhibitors GW4869. We found that both eHSP90α and EMT protein markers were regulated by GW4869 in a dose-dependent manner. GW4869 inhibited TGF-β1-induced eHSP90α expression and EMT protein markers, as well as suppressing TGF-β1-induced cell invasion and migration. So, the exosome inhibitor GW4869 can inhibit the expression of eHSP90α, EMT and invasion and migration of cells, which suggests that eHSP90α may promote the EMT and cell invasion and migration in gefitinib-sensitive NSCLC. Since it has been shown that extracellular HSP90α can be transported by exosomes, we treated cells with GW4869 and found it inhibit EMT and their ability to invade and migrate. Therefore, the high expression of HSP90α in the serum of NSCLC patients with EGFR mutation suggests that HSP90α is involved in the pathogenesis of NSCLC mutation,

while GW4869 can inhibit the expression of eHSP90α, suggesting that GW4869 may be a novel antitumor drug target.

EMT is considered as a key candidate for drug discovery against tumor. Epidermal growth factor-containing fibulin-like extracellular matrix protein 2(EFEMP2), a member of fibulin glycoprotein family, inhibits the invasion of lung cancer cells by inhibiting EMT and downregulating MMPs[37]. Cyclin-dependent kinase 7 (CDK7) inhibitors can play a role against EMT-mediated EGFR-TKIs resistance in NSCLC[38]. Diphenyl urea derivative (DUD) inhibited lung cancer cells migration by reversing EMT via Wnt/β-catenin and PI3K/Akt signaling and decrease in MMPs[39]. Namely, EMT endorses tumor cells with the ability to invade, migrate and resistance. Our wound healing assay and Transwell assay showed that hrHSP90α promoted the migration and invasion ability of TGF-β1-induced EMT cells in EGFR-mutated NSCLC cells. The invasion and migration of the TGF-β1-induced EMT model were inhibited by GW4869. These results also suggest that GW4869 hampered abilities of the tumor invasion and migration, which may provide a potential effect on EGFR-mutated invasion and migration. Meanwhile, we treated nude mice with gefitinib and GW4869 and preliminarily concluded that GW4869 can enhance the efficacy of gefitinib in inhibiting tumor growth. This tumor growth inhibition may be explained by the reduction in the level of eHSP90α. Interestingly, gefitinib combined with GW4869 was more effective than gefitinib alone, suggesting that GW4869 may enhance gefitinib sensitivity.

Conclusion

In conclusion, our results demonstrated that extracellular HSP90α induces epithelial-mesenchymal transition, promotes tumor cell invasion/migration, and GW4869 can inhibit epithelial-mesenchymal transition promoted by extracellular HSP90α in NSCLC cells. Thus, these findings may provide new strategies for delaying the development of acquired resistance to gefitinib in EGFR-mutated NSCLC.

Methods

Cell Lines and reagents. HCC827 cells (EGFR exon 19 deletion) was obtained from the American Type Culture Collection (USA). PC9 cells was from the Guangdong Lung Cancer Institute. We purchased gefitinib (ZD1839), GW4869 (S7609) from Selleck Chemicals (Houston, TX, USA). Recombinant transforming growth factor-β1 (TGF-β1) was purchased from R&D Systems (Minneapolis, MN, USA). Human recombinant HSP90α (hrHSP90α) was obtained from StressMarq Biosciences, Inc. (Victoria, BC, Canada).

Clinical specimens. This study was approved by the Ethics Committee of the Nanfang Hospital, Southern Medical University in Guangzhou, China (Medical Ethics No.NFEC-2019-065). The serum samples of 22 patients diagnosed with NSCLC EGFR mutation and 10 healthy adults were collected from Nangfang Hospital. Written informed consent was obtained from all of the participants in this study. Blood samples were collected by EDTA anticoagulation tube and carried to the laboratory where they were centrifuged at 3000 rpm for 10 min at 4℃. All of the samples were separated in EP tubes and stored at -80℃ until use.

The concentration of HSP90α in serum of the participants was determined by enzyme-linked immunosorbent assay (ELSIA). All of the research was carried out in accordance with the provisions of the Helsinki Declaration of 1975.

Plasmids, siRNAand transfection. The short interferingRNA(siRNA) and negative control siRNA targeting HSP90α were designed and synthesized by Genepharma (China). siHSP90α: sense(5'-3')GGUGCAGAUAUCUCUAUGATT, antisense(5'-3')UCAUAGAGAUAUCUGCACCTT. Transfections were performed with Lipofectamine 3000 reagent (Thermofisher, US) under the experimental procedure described above.

Western Blot. Protein lysate supernatants in radio immunoprecipitation Assay(RIPA) were collected and mixed with SDS-PAGE loading buffer. Total proteins in loading buffer were separated in 10% SDS-PAGE gels and transferred to a polyvinylidene difluoride (PVDF) membrane (Millipore Sigma, US). The membrane was blocked with 5% nonfat dry milk in tris-buffered saline supplemented with 20%TBS Tween 20 (TBST).The membrane was blocked with 5% nonfat dry milk in tris-buffered saline and Polysorbate 20 (TBST) and then probed with antibodies against HSP90α, E-cadherin, N-cadherin, (from Cell Signaling Technology, Danvers, MA, USA);Vimentin (Abcam, Cambridge, UK); and β-actin (Proteintech, Chicago, IL, USA).

Wound Healing Assay. Cells were seeded at an optimal density (5×10^5/ml) in a 6-well cell culture plate and incubated for 24 hours to 80% confluency. A 200 μL pipette tip was used to create a gap in the cell monolayer in each well, and each gap was then measured using an optical microscope. The monolayer was washed with a culture medium to remove cell debris, and then cells were allowed to migrate for 24 hours. Next, re-measured each gap under the optical microscope. The ratio of gap size after 24 hours to gap size at baseline was treated as the relative migration rate and analyzed using Image J.

Transwell Invasion Assay. Matrigel (Corning, US) was melted at 4°C and diluted to in growth medium at a ratio of 1:8. The diluted Matrigel was then added to coat the upper surface of the Transwell chambers (Corning, USA) at 30 μL per well. Cells (7×10^4) were then seeded in the coated membrane and the chambers placed into a Costar Transwell chamber plate containing growth medium. After 24 hours, cells in the upper side of the membrane were removed prior to staining. The Transwell chambers were removed and the medium was discarded. The chambers were then washed twice with PBS precooled at 4℃. Following, the PBS was discarded, and the chambers were placed in 4% paraformaldehyde for 20 min and then washed twice with PBS. Cells on the submembrane surface were stained using 0.1% crystal violet. Cells were counted in three randomly selected fields, and images were obtained under a microscope at 10× magnification. Then, we calculated the number of cells that had passed through the membrane.

Xenograft Model. BALB/C nude mice (male, 15–20g, 4–6 weeks old) were purchased from Laboratory Animal Center, the Southern Medical University, and housed in a dedicated specific-pathogen-free (SPF) facility. Mice were kept on a 12h light/dark cycle in an atmosphere of 40–70% humidity and average

temperature of about 24°C. All of the studies were performed following guidelines approved by the Institutional Animal Ethics Committee of Southern Medical University(Decision of laboratory animal ethics resolution No.L2019153). All animal experiments in this study complied with Animal Research, Reporting of *In Vivo* Experiments (ARRIVE) guidelines[40].

HCC827 cells (5×10^6) were subcutaneously injected into the mice's left flanks. After tumor size reached 50 mm^3, mice were randomly divided into three groups (n = 5 each): (1) Control group (treated with 0.5% CMC-Na, which was used as a vehicle for GW4869 and Gefitinib). (2) The gefitinib (20 mg/kg) group. (3) The combined GW4869 (12 μg/g) + Gefitinib (20 mg/kg) group. Mice received all abovementioned drugs intragastrically (i.g.) once a day. On the 28th day, mice were sacrificed. Blood samples were taken from mouse eyes. Immunohistochemistry (IHC) was performed on tumor tissues to assess the levels of E-cadherin and Vimentin.

Statistical Analysis. All data analyses were performed independently using GraphPad Prism software version 5.0 (GraphPad Software, USA). All data are expressed as mean ± standard deviation (SD). One-way ANOVA-Newman-Keults test was used to define statistical significance. $P < 0.05$ was considered statistically significant.

Declarations

Data availability

The data used or analysed support the findings of this study are available from the corresponding author on reasonable request.

Acknowledgments

This study was supported by the National Natural Science Foundation of China (81470228, 81670026) and Natural Science Foundation of Guangdong Province (2017A030313849). Sincerely thanks to the generous donation of PC9 from the Guangdong Lung Cancer Institute.

Author contributions

S.X.C. and H.M.D. designed of the work and wrote the manuscript; X.W. contributed to executing the experiments and wrote the manuscript; J.Z.D. and Y.T.F. performed data acquisition and interpretation; D.H.H. were responsible for analysis; All authors reviewed and approved the final manuscript.

Competing interests

The authors declare no conflict of interest.

References

1. Sung, H. et al. Global Cancer Statistics 2020: GLOBOCAN Estimates of Incidence and Mortality Worldwide for 36 Cancers in 185 Countries. CA Cancer J Clin. **71**, 209–249 (2021).
2. Ke, E. E., Zhou, Q. & Wu, Y. L. Emerging Paradigms in Targeted Treatments for Asian Patients with NSCLC. Expert Opin Pharmacother. **16**, 1167–1176 (2015).
3. Wu, S. G. & Shih, J. Y. Management of Acquired Resistance to EGFR TKI-targeted Therapy in Advanced Non-Small Cell Lung Cancer. Mol. Cancer. **17**, 38 (2018).
4. Esposito, A. R. et al. Liquid Biopsy Testing Can Improve Selection of Advanced Non-Small-Cell Lung Cancer Patients to Rechallenge with Gefitinib. Cancers (Basel). **11**, (2019).
5. Yoda, S., Dagogo-Jack, I. & Hata, A. N. Targeting Oncogenic Drivers in Lung Cancer: Recent Progress, Current Challenges and Future Opportunities. Pharmacol Ther. **193**, 20–30 (2019).
6. Gelatti, A., Drilon, A. & Santini, F. C. Optimizing the Sequencing of Tyrosine Kinase Inhibitors (TKIs) in Epidermal Growth Factor Receptor (EGFR) Mutation-Positive Non-Small Cell Lung Cancer (NSCLC). Lung Cancer. **137**, 113–122 (2019).
7. Gao, J., Li, H. R., Jin, C., Jiang, J. H. & Ding, J. Y. Strategies to Overcome Acquired Resistance to EGFR TKI in the Treatment of Non-Small Cell Lung Cancer. Clin. Transl. Oncol. **21**, 1287–1301 (2019).
8. Jolly, M. K. & Celia-Terrassa, T. Dynamics of Phenotypic Heterogeneity Associated with EMT and Stemness during Cancer Progression. J Clin Med. **8**, (2019).
9. Shibue, T. & Weinberg, R. A. EMT, CSCs, and Drug Resistance: The Mechanistic Link and Clinical Implications. Nat. Rev. Clin. Oncol. **14**, 611–629 (2017).
10. Delahaye, C. et al. Early Steps of Resistance to Targeted Therapies in Non-Small-Cell Lung Cancer. Cancers (Basel). **14**, (2022).
11. Jakobsen, K. R., Demuth, C., Sorensen, B. S. & Nielsen, A. L. The Role of Epithelial to Mesenchymal Transition in Resistance to Epidermal Growth Factor Receptor Tyrosine Kinase Inhibitors in Non-Small Cell Lung Cancer. Transl Lung Cancer Res. **5**, 172–182 (2016).
12. Nowak, E. & Bednarek, I. Aspects of the Epigenetic Regulation of EMT Related to Cancer Metastasis. *Cells*. **10**, (2021).
13. Lang, B. J. et al. Heat Shock Proteins are Essential Components in Transformation and Tumor Progression: Cancer Cell Intrinsic Pathways and Beyond. Int. J. Mol. Sci. **20**, (2019).
14. Dong, H. M. et al. Extracellular Heat Shock Protein 90Alpha Mediates HDM-induced Bronchial Epithelial Barrier Dysfunction by Activating RhoA/MLC Signaling. Respir Res. **18**, 111 (2017).
15. Hoter, A., El-Sabban, M. E. & Naim, H. Y. The HSP90 Family: Structure, Regulation, Function, and Implications in Health and Disease. Int. J. Mol. Sci. **19**, (2018).
16. Wong, D. S. & Jay, D. G. Emerging Roles of Extracellular Hsp90 in Cancer. Adv. Cancer Res. **129**, 141–163 (2016).
17. Taha, E. A., Ono, K. & Eguchi, T. Roles of Extracellular HSPs as Biomarkers in Immune Surveillance and Immune Evasion. Int. J. Mol. Sci. **20**, (2019).

18. Den RB & Lu, B. Heat Shock Protein 90 Inhibition: Rationale and Clinical Potential. Ther Adv Med Oncol. **4**, 211–218 (2012).
19. Li, W. et al. Extracellular Hsp90 (eHsp90) as the Actual Target in Clinical Trials: Intentionally Or Unintentionally. Int Rev Cell Mol Biol. **303**, 203–235 (2013).
20. Eguchi, T., Taha, E. A., Calderwood, S. K. & Ono, K. A Novel Model of Cancer Drug Resistance: Oncosomal Release of Cytotoxic and Antibody-Based Drugs. Biology (Basel). **9**, (2020).
21. Catalano, M. & O'Driscoll, L. Inhibiting Extracellular Vesicles Formation and Release: A Review of EV Inhibitors. J Extracell Vesicles. **9**, 1703244 (2020).
22. Li, X. Q. et al. Exosomes Derived From Gefitinib-Treated EGFR-mutant Lung Cancer Cells Alter Cisplatin Sensitivity Via Up-Regulating Autophagy. Oncotarget. **7**, 24585–24595 (2016).
23. Hayatudin, R. et al. Overcoming Chemoresistance Via Extracellular Vesicle Inhibition. Front Mol Biosci. **8**, 629874 (2021).
24. Chen, R. et al. Exosomes-Transmitted miR-7 Reverses Gefitinib Resistance by Targeting YAP in Non-Small-Cell Lung Cancer. Pharmacol. Res. **165**, 105442 (2021).
25. Eguchi, T. et al. Cell Stress Induced Stressome Release Including Damaged Membrane Vesicles and Extracellular HSP90 by Prostate Cancer Cells. Cells. **9**, (2020).
26. Lin, Y., Wang, X. & Jin, H. EGFR-TKI Resistance in NSCLC Patients: Mechanisms and Strategies. Am. J. Cancer Res. **4**, 411–435 (2014).
27. Poggio, P., Sorge, M., Secli, L. & Brancaccio, M. Extracellular HSP90 Machineries Build Tumor Microenvironment and Boost Cancer Progression. Front Cell Dev Biol. **9**, 735529 (2021).
28. Du Y, Wu, J. & Luo, L. Secreted Heat Shock Protein 90alpha Attenuated the Effect of Anticancer Drugs in Small-Cell Lung Cancer Cells through AKT/GSK3beta/beta-Catenin Signaling. Cancer Control. **25**, 1146239753 (2018).
29. Hashida, S. et al. Hsp90 Inhibitor NVP-AUY922 Enhances the Radiation Sensitivity of Lung Cancer Cell Lines with Acquired Resistance to EGFR-tyrosine Kinase Inhibitors. Oncol. Rep. **33**, 1499–1504 (2015).
30. Yu, J., Zhang, C. & Song, C. Pan- and Isoform-Specific Inhibition of Hsp90: Design Strategy and Recent Advances. Eur. J. Med. Chem. **238**, 114516 (2022).
31. Birbo, B., Madu, E. E., Madu, C. O., Jain, A. & Lu, Y. Role of HSP90 in Cancer. Int. J. Mol. Sci. **22**, (2021).
32. Lauwers, E. et al. Hsp90 Mediates Membrane Deformation and Exosome Release. Mol. Cell. **71**, 689–702 (2018).
33. Essandoh, K. et al. Blockade of Exosome Generation with GW4869 Dampens the Sepsis-Induced Inflammation and Cardiac Dysfunction. Biochim Biophys Acta. **1852**, 2362–2371 (2015).
34. You, J. et al. Snail1-Dependent Cancer-Associated Fibroblasts Induce Epithelial-Mesenchymal Transition in Lung Cancer Cells Via Exosomes. QJM. **112**, 581–590 (2019).

35. Chen, J. et al. The Exosome-Like Vesicles Derived From Androgen Exposed-Prostate Stromal Cells Promote Epithelial Cells Proliferation and Epithelial-Mesenchymal Transition. Toxicol Appl Pharmacol. **411**, 115384 (2021).
36. Yang, Y. et al. Exosomal PD-L1 Harbors Active Defense Function to Suppress T Cell Killing of Breast Cancer Cells and Promote Tumor Growth. Cell Res. **28**, 862–864 (2018).
37. Song, L. et al. EFEMP2 Suppresses the Invasion of Lung Cancer Cells by Inhibiting Epithelial-Mesenchymal Transition (EMT) and Down-Regulating MMPs. Onco Targets Ther. **13**, 1375–1396 (2020).
38. Ji, W. et al. Efficacy of the CDK7 Inhibitor On EMT-Associated Resistance to 3Rd Generation EGFR-TKIs in Non-Small Cell Lung Cancer Cell Lines. Cells. **9**, (2020).
39. Dai, B. et al. Novel Diphenyl Urea Derivative Serves as an Inhibitor On Human Lung Cancer Cell Migration by Disrupting EMT Via Wnt/beta-catenin and PI3K/Akt Signaling. Toxicol. In Vitro. **69**, 105000 (2020).
40. McGrath, J. C. & Lilley, E. Implementing Guidelines On Reporting Research Using Animals (ARRIVE Etc.): New Requirements for Publication in BJP. Br J Pharmacol. **172**, 3189–3193 (2015).

Figures

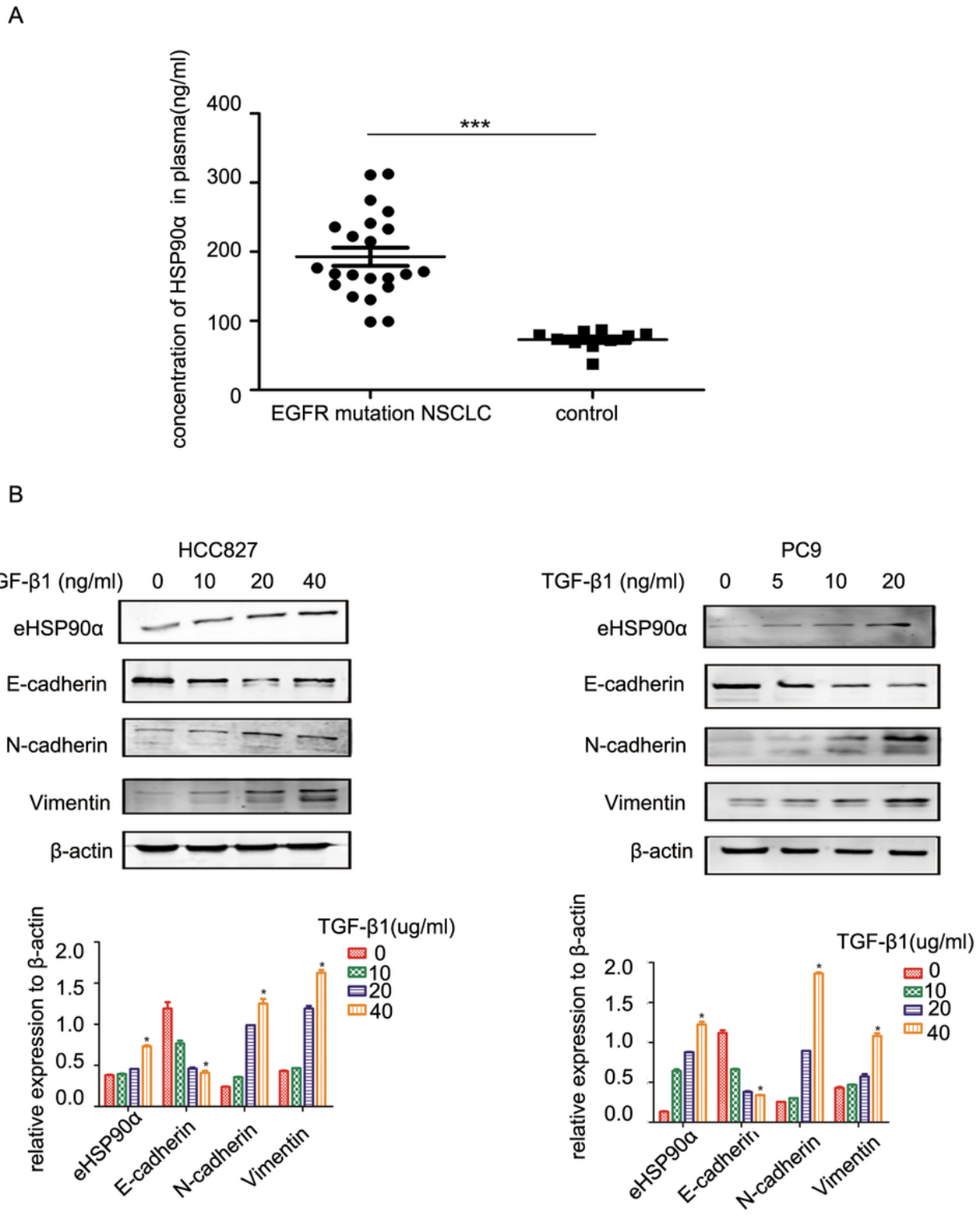

Figure 1

Expression of HSP90α in plasma levels and NSCLC cells.

(A) Secretion of HSP90α in plasma samples from EGFR-mutated NSCLC patients (n = 22) and healthy patients (n = 10) was assessed by ELISA. ***$P < 0.001$ *vs.* control. (B) HCC827 was treated with TGF-β1

for 24 hours and PC9 was treated with TGF-β1 for 6 hours. Expression of eHSP90α, E-cadherin, N-cadherin and vimentin in NSCLC cells was detected by WB.*$P < 0.05$ *vs.* control.

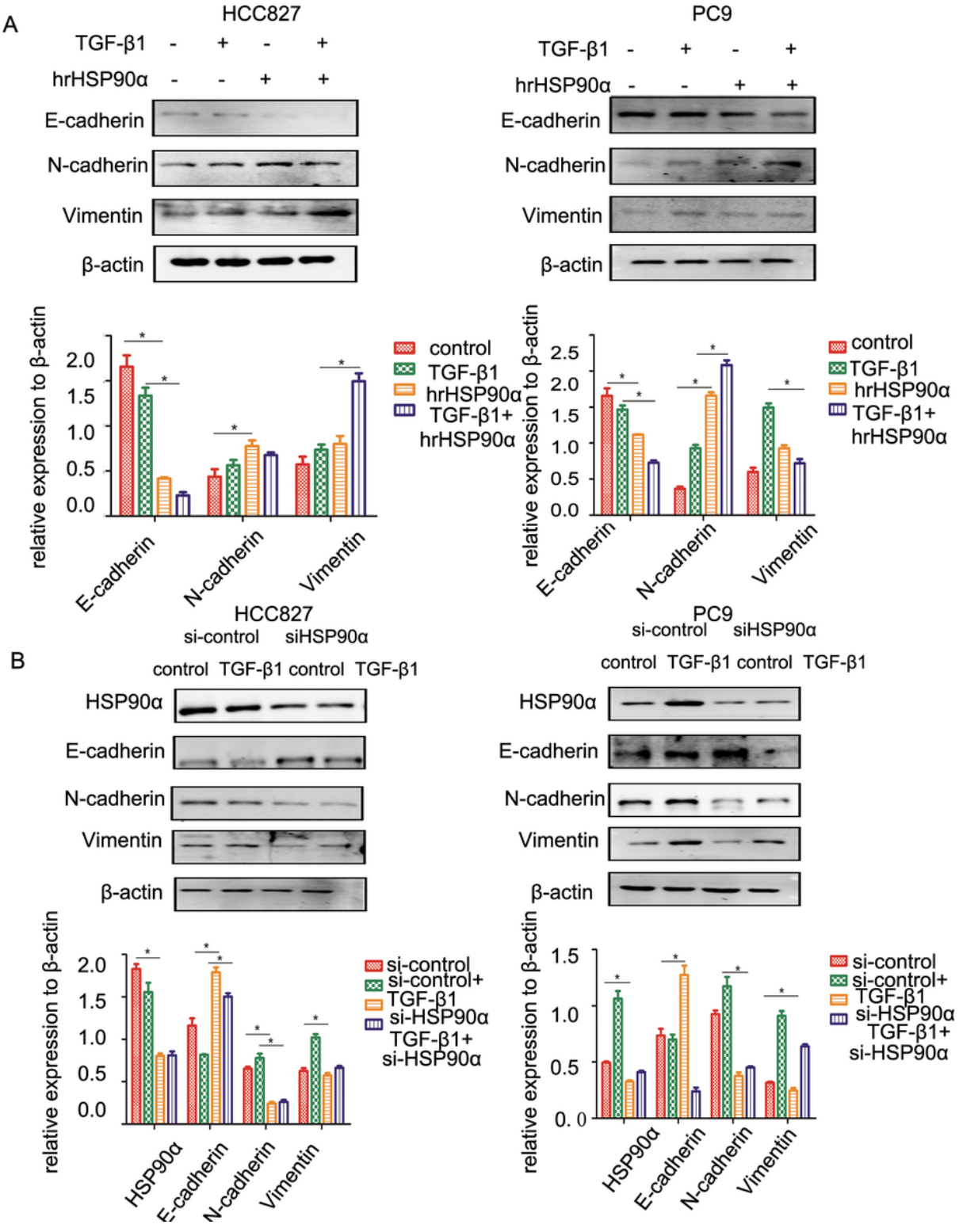

Figure 2

eHSP90α promote epithelial-mesenchymal transition.

(A) HCC827 was treated with TGF-β1 and hrHSP90α for 24 hours and PC9 was treated with TGF-β1 and hrHSP90α for 6hours. Expression of E-cadherin, N-cadherin and vimentin was detected by western blot. *P < 0.05. (B) si-Control and si-HSP90α were treated with TGF-β1+ HSP90α. Expression of E-cadherin, N-cadherin and vimentin as detected by western blot.*P < 0.05.

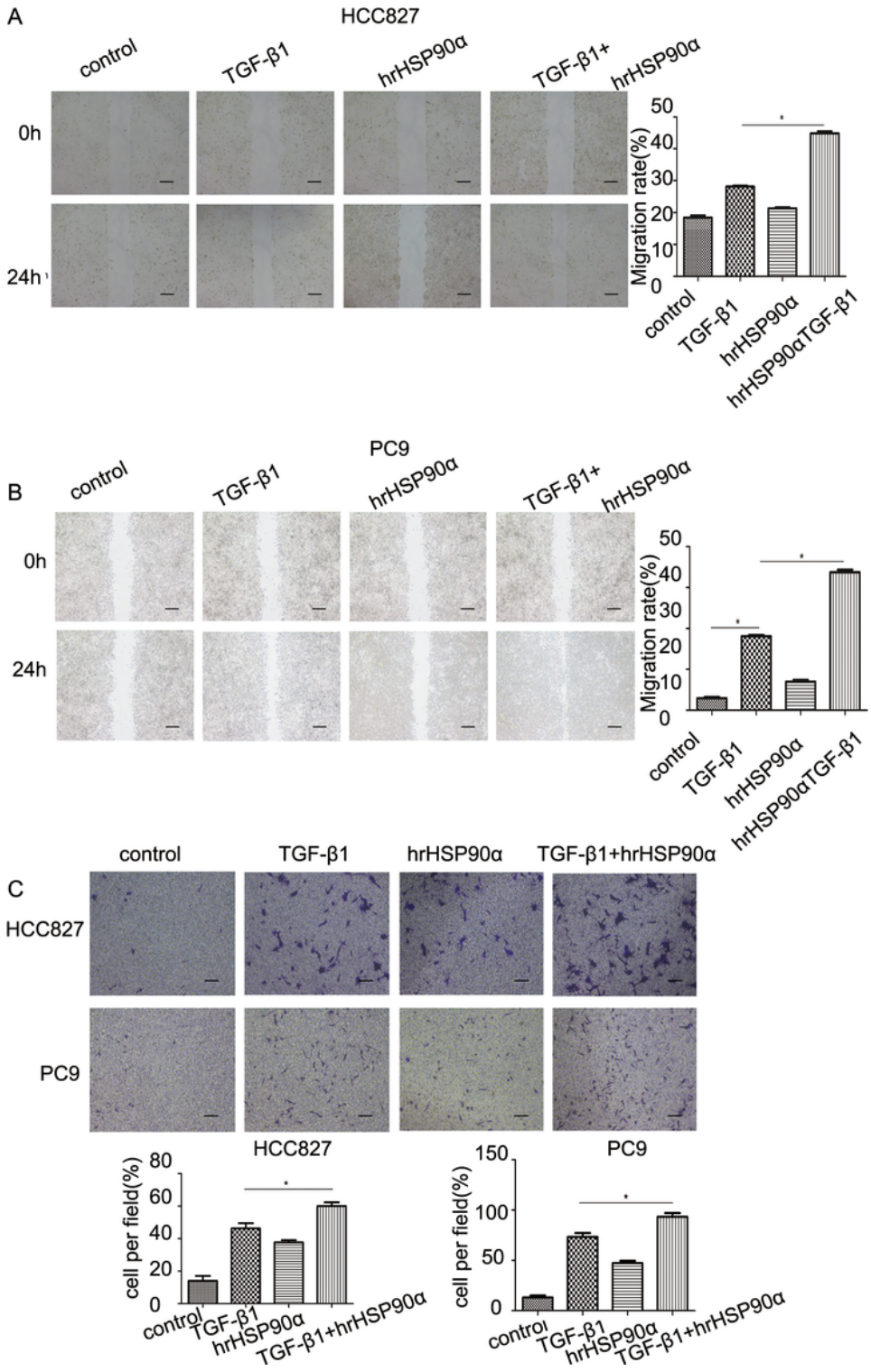

Figure 3

eHSP90α accelerated invasion/migration abilities of NSCLC cells.

(A-B) Migration rates with the treatment of TGF-β1 and hrHSP90α were measured by wound healing. (magnification: ×10; scale bar: 5 μm). *P < 0.05. (C) Invasion rates with the treatment of TGF-β1 and hrHSP90α were measured by transwell assays (magnification: ×10; scale bar: 5 μm). *P < 0.05. Data shown are the mean± SD of three independent trials.

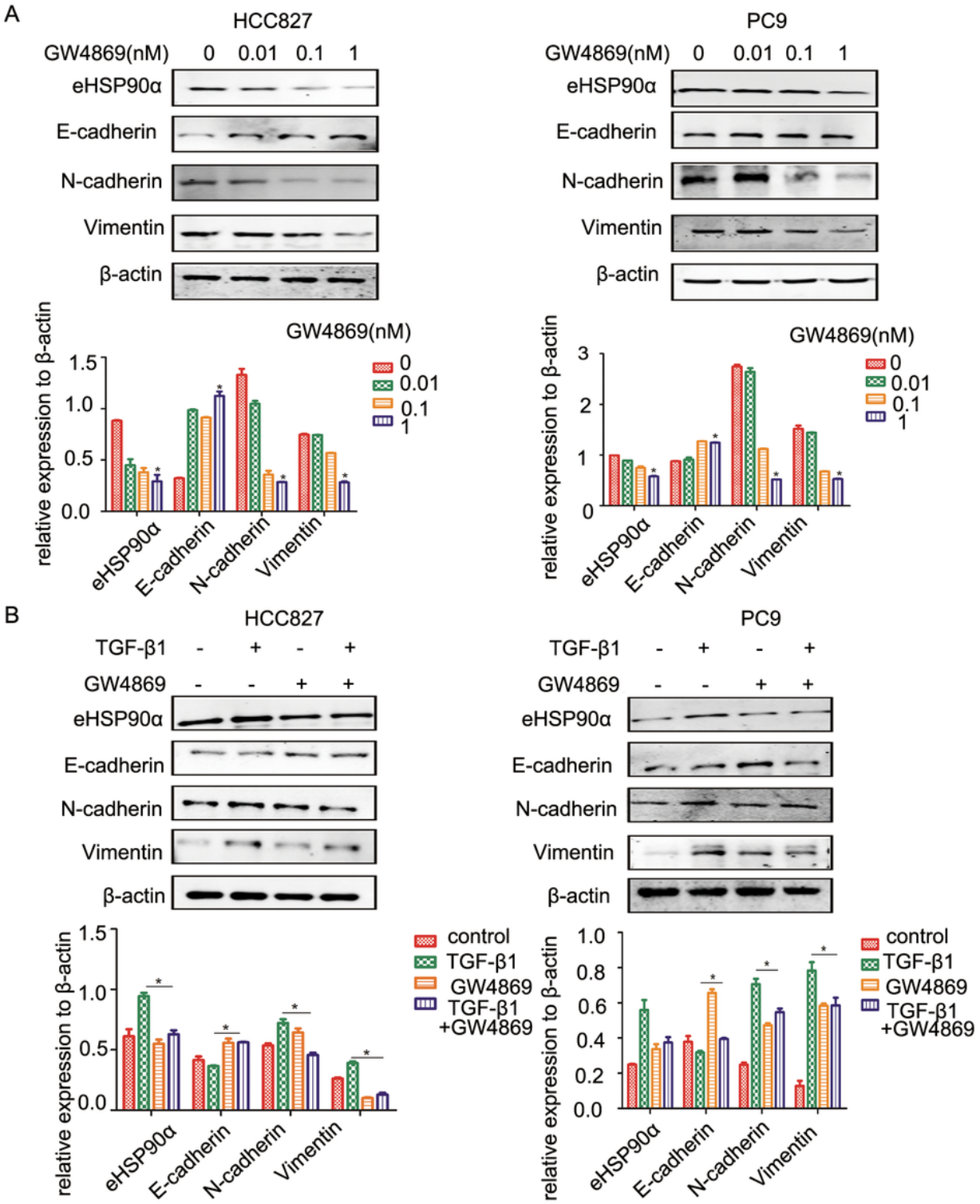

Figure 4

GW4869 inhibited eHSP90α release and epithelial mesenchymal transition.

(A) Expression of eHSP90α, E-cadherin, N-cadherin and Vimentin with the treatment of GW4869 was detected by western blot.*$P < 0.05$ *vs.* control. (B) Western blot shows the expression of eHSP90α, E-cadherin, N-cadherin and Vimentin in the combination of GW4869 and TGF-β1 .*$P < 0.05$.

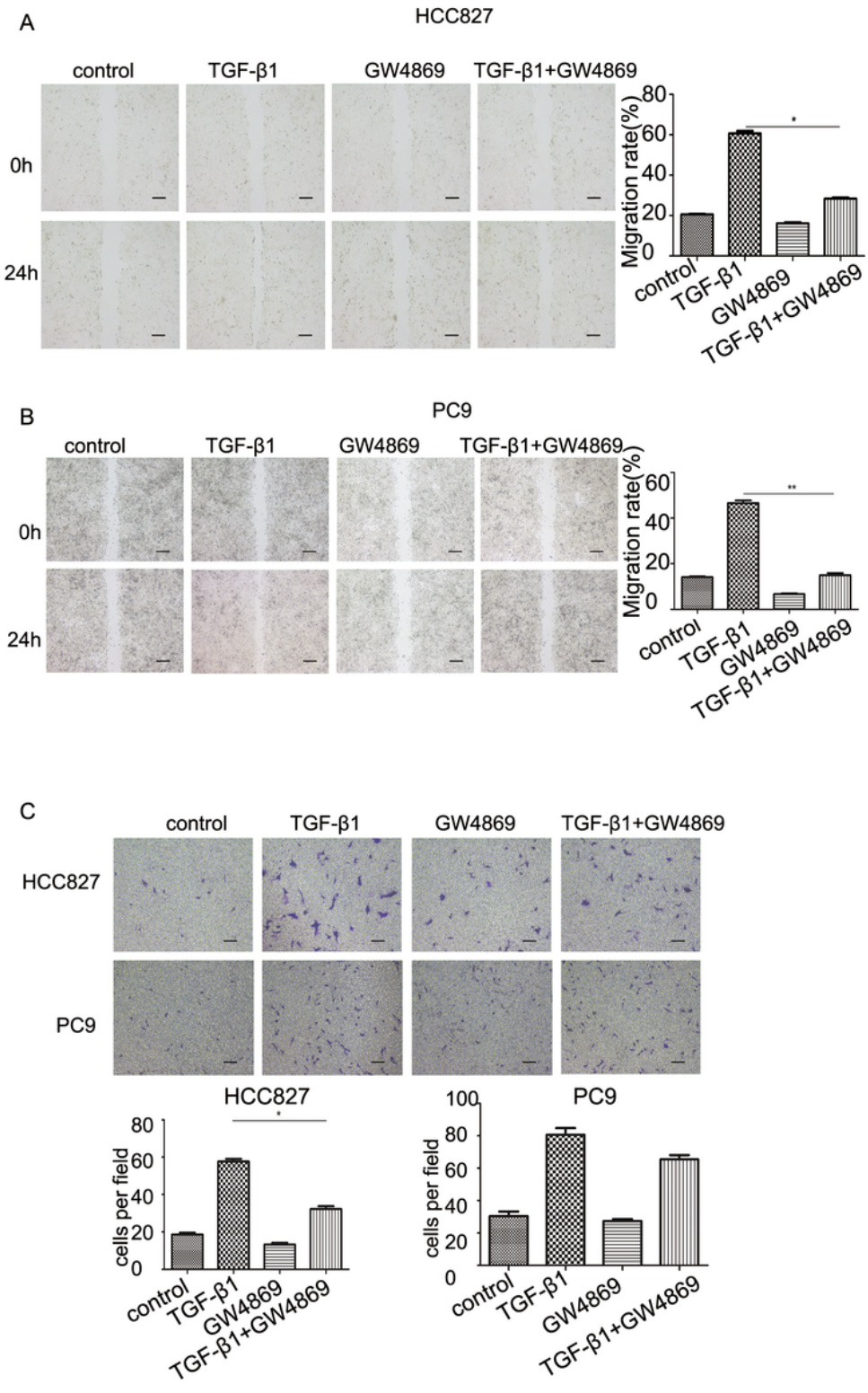

Figure 5

GW4869 inhibited invasion/migration abilities in NSCLC cells

(A-B) Migration rates under the treatment of TGF-β1 and GW4869 were measured by wound healing. (magnification: ×10; scale bar: 5 μm). *P < 0.05. (C) Invasion rates under the treatment of TGF-β1 and GW4869 were measured by transwell assays (magnification: ×10; scale bar: 5 μm). *P < 0.05. Data shown are the mean± SD of three independent trials.

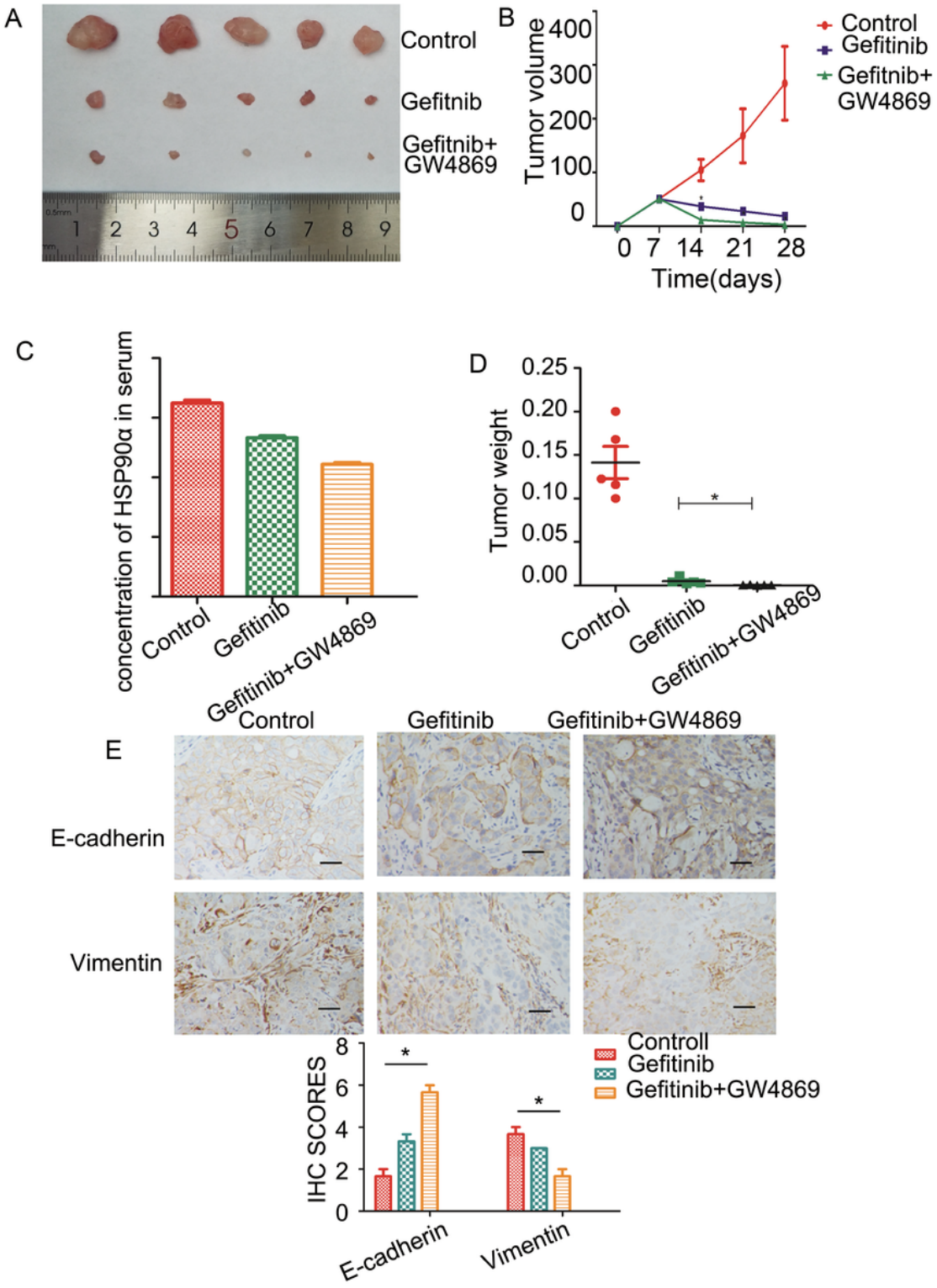

Figure 6

GW4869 enchances gefitinib sensitivity in BALB/C mice *in vivo.*

(A) The tumor size of three groups (control, gefitinib, GW4869 +gefitinib). (B) The tumor volumes were measured at the day 28 .*$P < 0.05$,versus Gefitinib. (C) The concentration of HSP90α in the serum of mice was detected by ELISA . (D) Tumor weight between the group of gefitinib and gefitinib+GW4869. (E) The

expression of E-cadherin and Vimentin were analyzed by immunohistochemistry (magnification:×40; scar bar:20μm) and the IHC-SCORES of E-cadherin and Vimentin was shown.*$P < 0.05$. Data shown are the mean± SD of three independent trials.

Supplementary Files

This is a list of supplementary files associated with this preprint. Click to download.

- Originalgelswcs.pdf